Fatigue Strength and Fracture Behaviour of CHS-to-RHS T-Joints Subjected to Out-of-Plane Bending

Li-Chun Bian

College of Mechanical and Power Engineering, Nanjing University of Technology Nanjing, Jiangsu 210009, People's Republic of China

Jae-Kyoo Lim*, Yon Jig Kim

Department of Mechanical Design, Automobile Hi-Technology Research Center, Chonbuk National University, Chonju, Chonbuk 561-756, Korea

The fatigue behaviour of six different hollow section T-joints subjected to out-of-plane bending moment was investigated experimentally using scaled steel models. The joints had circular brace members and rectangular chord members. Hot spot stresses and the stress concentration factors (SCFs) were determined experimentally. Fatigue testing was carried out under constant amplitude loading in air. The test results have been statistically evaluated, and show that the experimental SCF values for circular-to-rectangular (CHS-to-RHS) hollow section joints were found to be below those of circular-to-circular (CHS-to-CHS) hollow section joints. The fatigue strength, referred to experimental hot spot stress, was in reasonably good agreement with referred fatigue design codes for tubular joints.

Key Words : Hollow Section, Welded Joint, Fatigue, Hot Spot Stress, Stress Concentration Factor

Nomenclature

d	: Outside diameter of brace
l	: Length of brace
t	: Thickness of brace
AWS	: American Welding Society
B	: Outside width of chord
DEn	: Department of Energy, UK
DnV	: Det norske Veritas
E	: Young's modulus of elasticity
OPB	: Out-of-plane bending loading
L	: Length of chord
N	: Cycle number (fatigue life)
R	: Stress ratio, S_{min}/S_{max}
SCF	: Stress concentration factor
S_{max}	: Maximum nominal stress in a constant amplitude cycle
S_{min}	: Minimum nominal stress in a constant amplitude cycle
S_{HS}	: Hot spot stress
S_{nom}	: Brace nominal stress (according to beam theory)
T	: Thickness of chord
$\alpha, \beta, \gamma, \tau$	: Non-dimensional geometrical parameters, see Fig. 1 and Table 2
$\Delta S_{H.S}$	: Hot spot stress range
ΔS_{nom}	: Brace nominal stress range
ε_{HS}	: Extrapolated hot spot strain
S_{YS}	: Minimum specified yield stress

* Corresponding Author,
E-mail : jklim@moak.chonbuk.ac.kr
TEL : +82-63-270-2321; **FAX :** +82-63-270-2460
Department of Mechanical Design, Automobile Hi-Technology Research Center, Chonbuk National University, Chonju, Chonbuk 561-756, Korea. (Manuscript **Received** April 20, 2002; **Revised** October 30, 2002)

1. Introduction

The fatigue failure of hollow section joints is commonly encountered in dealing with engineering structures. It is found that the fatigue failure of practical structures, in general, first occurs at the weld toe of the joints. The static and fatigue assessment of hollow section weld joints is of great importance in ensuring structural reliability

and has been given special attention by many investigators (Chiew and Soh, 2000; Suh et al., 2001). Hollow section joints are generally either circular-to-circular (CHS-to-CHS) or rectangular-to-rectangular (RHS-to-RHS) joints. For offshore structures, which are subjected to fatigue by wave loading, circular hollow sections are used almost exclusively due to their relatively smaller hydrodynamic loads and stress concentrations in joints. However, in CHS-to-CHS joints, the hollow section members are joined together by welding the profiled ends of secondary members, the braces, onto the circumference of the main member, the chord. Therefore, compared with RHS-to-RHS joints, the fabrication of CHS-to-CHS joints is more costly due to their complicated joint geometry. Also, the behaviour of these welded tubular connections, even in their simplest configuration, is complex and their analysis is difficult. The stress concentrations in RHS-to-RHS joints are generally larger, and they have correspondingly lower fatigue lives. However, rectangular hollow sections provide a simpler joint geometry for fabrication of the joints (lower joint fabrication cost) and are frequently used for onshore structures and structures which are predominantly subjected to static loads. Joints with circular braces and rectangular chords may in many applications provide an optimum solution with a simple joint geometry for fabrication and a relatively smaller stress concentration factor compared to RHS-to-RHS joints. However, a study of the available literature reveals that there is a very little information and virtually no design guidance available for the fatigue design of CHS-to-RHS joints. The current lack of design recommendations has been a major obstacle to the use of this hybrid connection for fatigue-loaded structures.

Bian and Lim (2001) presented some experimental results for CHS-to-RHS joints with axial and in-plane bending loadings, which indicated that joints with a large β-ratio would fail with anomalously low fatigue strength. The stress concentration factors (SCFs) for this hybrid joint (CHS-to-RHS) were sometimes between those of the RHS-to-RHS joint and the CHS-to-CHS

joint, and sometimes even below the CHS-to-CHS joint. The mean fatigue life correlated well with the proposed design curve for 16 mm plate thickness (Gurney, 1982). Therefore, it appeared worthwhile doing more investigations on CHS-to-RHS joints. In the present study, the fatigue behaviour of CHS-to-RHS T-joints subjected to out-of-plane bending loading was investigated experimentally, and the results obtained were compared with design guidance for CHS-to-CHS joints. Some of the specimens were joints with a large β-ratio. The work was undertaken in order to provide a data base which could be developed into design guidance for fatigue design of CHS-to-RHS joints. This study is a basic, and also a necessary, step for the practical application of CHS-to-RHS joints and forms a foundation for future studies.

2. Experimental Specimens

The material of the brace and chord members was steel to Standard DIN 17100, which is commonly used in offshore structures and has the following nominal tensile properties,

Modulus of Elasticity, E : 210 GPa
Min. Yield Stress, S_{YS} :   275 MPa
Min. Elongation :   22%

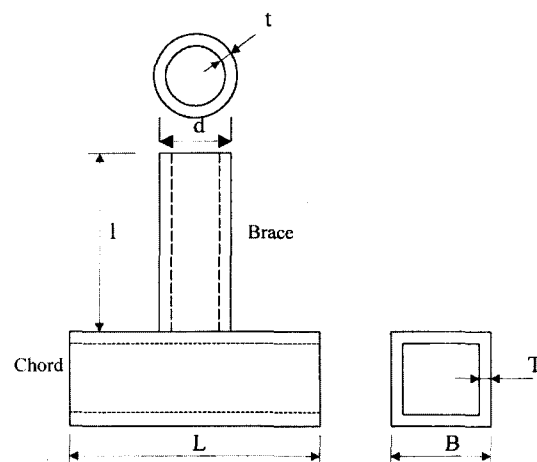Figure 1 illustrates a typical T-joint geometry used in the present experiments. The details of

Fig. 1   Geometry of a CHS-to-RHS joint

Table 1 Dimensions of specimens

Specimen No.	Brace			Chord		
	d (mm)	t (mm)	l (mm)	B (mm)	T (mm)	L (mm)
T1OPB	82.5	6.7	900	200	10.0	720
T2OPB	51.0	8.7	900	180	10.0	720
T3OPB	160.0	6.3	900	200	6.3	1000
T4OPB	82.5	6.7	900	200	10.0	1000
T5OPB	140.0	8.7	900	200	10.0	1200
T6OPB	160.0	6.3	900	200	6.3	1200

T : T-joint, OPB : out-of-plane bending loading.

Table 2 Non-dimensional geometrical parameters of the specimens

Specimen No.	α	β	γ	τ
T1OPB	3.60	0.41	10.00	0.67
T2OPB	4.00	0.28	9.000	0.87
T3OPB	5.00	0.80	15.90	1.00
T4OPB	5.00	0.41	10.00	0.67
T5OPB	6.00	0.70	10.00	0.87
T6OPB	6.00	0.80	15.90	1.00

where $\alpha=L/B$, $\beta=d/B$, $\gamma=B/2T$ and $\tau=t/T$.

the specimens are listed in Table 1. The main geometrical factors governing the fatigue behaviour can be expressed by the non-dimensional geometrical parameters as presented in Table 2. The specimens were fabricated locally by manual electric metal arc welding with full penetration welds. The welding procedures were the same as for offshore applications. The brace member was located at the mid section of the chord. The joints were inspected using standard non-destructive testing methods to ensure that no cracks or fabrication weld defects were present.

3. Experimental Set-up

For hollow section joints three different basic loading cases are defined: axial loading, in-plane and out-of-plane bending loadings. Each load case has its particular distribution of stresses along the intersection line and thereby its particular influence on the fatigue life of the joint. In the present investigation, six specimens were tested with out-of-plane bending moment. Figure 2 shows the experimental set-up. The both ends of
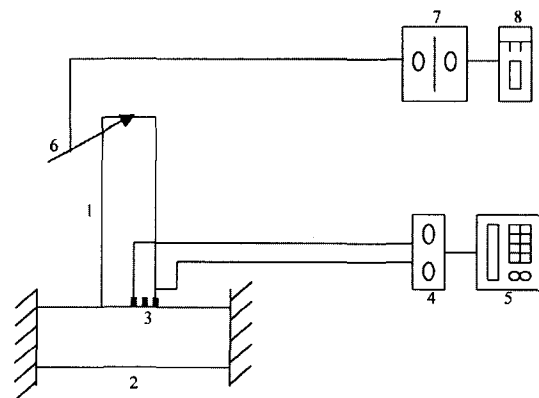

Fig. 2 Schematic diagram of the experimental system 1. Brace. 2. Chord. 3. Electric strain gauges. 4. Amplifier. 5. Strain logger. 6. Static/Fatigue loads. 7. Actuator control unit. 8. Fatigue cycle counter.

the chord were restrained rigidly in all directions. Static and fatigue loads were applied by loading at the end of the brace. The models were instrumented with strain gauges. Strains were measured in the static tests prior to fatigue loading. Loading was applied by a computer controlled servo-

hydraulic actuator system operated in load control.

4. Experimental Procedure

4.1 Static loading

The main purpose of conducting stress analyses of hollow section joints is to obtain information on the hot spot strain and hot spot stress (DEn, 1990 ; AWS, 1998) and, hence, the stress concentrations around the intersections for fatigue analysis. The hot spot stress is the stress in the most highly stressed region within the structure and is thought to best characterise fatigue in hollow section joints. The hot spot stress generally occurs at a discontinuity, such as the weld toe, where fatigue crack initiation can be expected to start. Prior to fatigue testing, all the specimens were instrumented with strain gauges to allow for the measurement of hot spot strains in both the brace and the chord. For a more local possibility, strain gauges of 1 mm length were used. The strains were measured along three different extrapolation lines (0°, 45° and 90°) on both the brace and the chord as shown in Figs. 3 and 4. Along each extrapolation line two strain gauges were located at distances 4 and 6 mm from the weld toe, respectively. A third gauge was located at a further distance of 1.0t/1.0T from the weld toe. The measured values were fitted to a quadratic curve using the least squares method, to obtain the strain gradient towards the weld toe of the joint. The hot spot strain was determined by extrapolating the measured strain values to the weld toe according to the DnV (Gibstein and Moe, 1985) and ECSC (Radenkovic, 1981) definitions of hot spot strain for tubular joints and by the quadratic extrapolation method (van Wingerde, 1992), respectively.

The joints were loaded statically in small increments to a hot spot strain value within the range of 500-1000 $\mu\varepsilon$ during the strain measurements. The strain gauge readings at each increment were noted. Prior to measuring strains the load was cycled 6-8 times to the same level for conditioning of specimens and strain gauges (to ensure the readings stabilized). This loading pro-
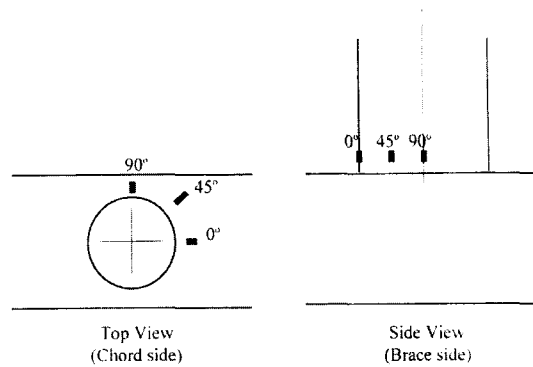
Top View   Side View
(Chord side)   (Brace side)

Fig. 3 Locations of strain gauges

Fig. 4 Locations of strain gauges on the specimen employed

cedure ensures a satisfactory performance of the strain gauges and eliminates the drift or any hysteresis of strain measurements due to the fabrication of the joints. In the static tests care was taken to avoid any loads above the load level of the ensuing fatigue test.

4.2 Fatigue tests

On the basis of measured SCF values for the joints, fatigue testing was carried out with constant amplitude sinusoidal loading in air and test frequencies in the range of 1.0-10.0 Hz, depending upon the magnitude of loading. The stress ratio was $R = -0.36$. In order to evaluate the influence of geometric parameters on fatigue strength, all the joints were tested at an ECSC (Radenkovic, 1981) hot spot stress range of approximately $\Delta S_{HS} = 300$ MPa. The fatigue test was continued until rupture of the joint (not complete rupture).

In the present investigation, the following three measures of fatigue life were recorded :

N_2-crack initiation,

N_3-through thickness crack,

N_4-rupture of joint.

Before commencing a test both the brace and the chord were sealed and pressurized to 1.5 bar. The detection of fatigue crack initiation was carried out visually by spraying white spirit on the surface of the joint. Initial cracks could be detected by observing the pumping of liquid in and out of the crack in phase with the loading. In most of the cases the initial cracks were detected when they were very small with a depth of the order of about 0.1 mm. By continuously monitoring the pressure inside the brace and the chord, through thickness cracking (N_3) could be detected with a good accuracy.

5. Results and Discussion

5.1 Static loading

After determining the extrapolated hot spot strains ε_{HS}, the stress concentration factors at the weld toe in both the brace and the chord for each specimen were determined by using the following equation,

$$SCF = \frac{S_{HS}}{S_{nom}} = \frac{E \cdot \varepsilon_{HS}}{S_{nom}} \qquad (1)$$

where S_{HS} is the hot spot stress, S_{nom} is the brace nominal stress and E is Young's Modulus of elasticity. Note that the actual cross section of the brace was used in the determination of the nominal stress.

In Table 3 the maximum SCFs calculated from parametric formulae are compared with experimental results. It should be noted that the UEG (1985), the DnV (1990) and Gibstein and Moe's formulae (1985) were derived for CHS-to-CHS joints. The Soh and Soh's formula (1989) was derived for joint geometries with square brace members and circular chord members, i.e., the opposite configuration compared to the present joint. As presented in Table 3, it is very interesting to note that the experimental SCFs of CHS-to-RHS joints exhibit a substantial improvement
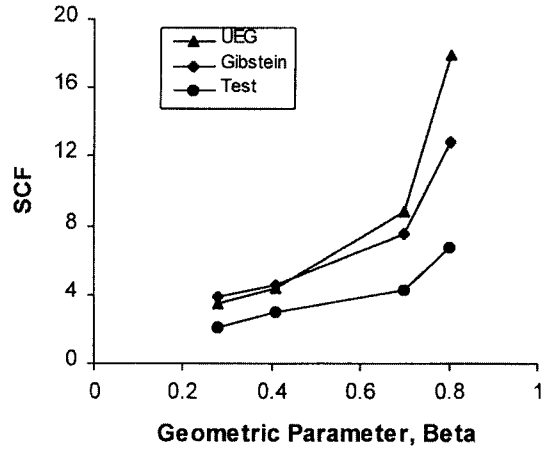

Fig. 5 Influence of β on SCFs from the present experiment and parametric formulae for out-of-plane bending
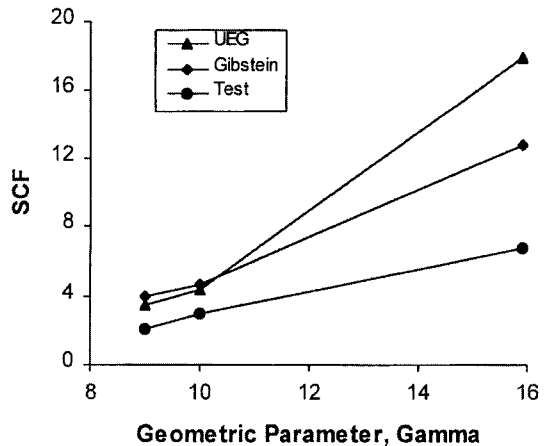

Fig. 6 Influence of γ on SCFs from the present experiment and parametric formulae for out-of-plane bending

compared to those of CHS-to-CHS joints. The Soh's formula, which was based on finite element analysis, appears to be suitable for CHS-to-RHS joints and can be approximately used to predict SCFs for CHS-to-RHS joints.

Figures 5-7 show the influence of the geometric parameters (β, γ and τ) on SCFs, and the experimental values of SCFs are compared with parametric formulae for a range of geometric parameters. As the α parameter does not appear in the relevant parametric equations, its influence on SCFs is not considered here.
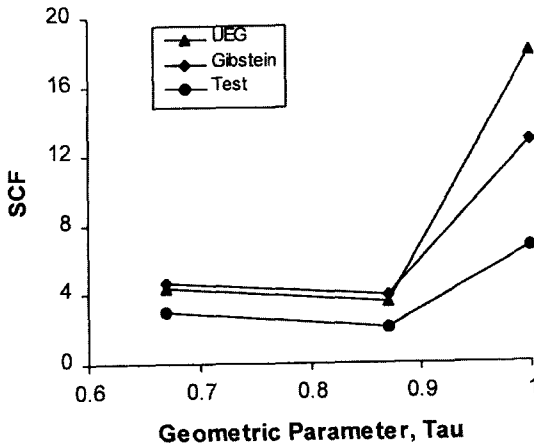
Fig. 7 Influence of τ on SCFs from the present experiment and parametric formulae for out-of-plane bending

As shown in Fig. 5, the experimental SCF values increase with the increase of β, but are below the values of CHS-to-CHS joints in all the cases. The parametric SCF values from UEG and Gibstein's formulae plotted on the same figure follow the same trend. The values from Gibstein's formula are relatively closer to the experimental values, and can be taken as the upper bound values for the CHS-to-RHS joints.

It can be seen from Fig. 6 that the experimental SCF values increase with the increase of γ. The parametric SCF values from UEG and Gibstein's formulae plotted on the same figure almost have the same trend, but increase more quickly compared to the CHS-to-RHS joints. The experimental SCF values tend to cover the lower bound values with the values from UEG formula covering the upper bound values.

As shown in Fig. 7, the experimental SCF values decrease slowly at first and then increase quickly with the increase of τ. The trend is in line the same as predicted SCF values from UEG and Gibstein's formulae. In all the cases, the SCF values of CHS-to-RHS joints are lower than those of CHS-to-CHS joints. As a result, the experimental SCF values of CHS-to-RHS joints exhibit a substantial improvement compared to those predicted from UEG and Gibstein's formulae for CHS-to-CHS joints.

5.2 Fatigue tests

During the fatigue tests, cracks initiated at the weld toe in the hot spot region, and the joints failed from the chord sides. The fatigue test results are summarised in Table 4. Note that in Table 3 the SCF value in specimen T6OPB is greater than that in specimen T5OPB. In general, the fatigue life (loading cycles) increases with decreasing the SCF value. However, it can be observed from Table 4 that the fatigue life of the specimen T6OPB is longer than that for specimen T5OPB. This turns out contrary to the knowledge. It has been known for a long time that the brace and the chord wall thicknesses influence the fatigue life of the joints. According to the experiments, the fatigue life of the joints decreases with increasing the brace or the chord wall thickness (DEn, 1990; AWS, 1998). Thus, in the authors' opinion, this anomalous case is probably due to the reason that both the brace and the chord wall thicknesses of the specimen T5OPB are relatively larger than those for specimen T6OPB. In Fig. 8 the fatigue test results (N_3) are compared with the DEn (Gurney, 1982) design curve and associated scatter band for tubular joints. The agreement between the test data and the DEn (Gurney, 1982) design curve appears to be fair. All the present test data fall above the design S-N curve and within the Mean ± 2 (Standard Deviations) scatterband. The mean value of N_3 is close to the mean S-N curve for joints with wall thickness in the range 16-32 mm.

5.3 Thickness effect

The thickness effect is one of the major influencing factors of fatigue strength of welded joints. It has been known for a long time that chord wall thickness influences the fatigue strength of tubular joints. According to the experiments, the fatigue strength of tubular joints decreases with increasing chord wall thickness. Such an effect has long been recognized in welded plates. However, thickness effect is a very complex phenomenon and its general rule and mechanism have not yet been sufficiently elucidated. In the present study, the welded plate thickness correction factor (Gurney, 1991) was adopted for all

Table 3 Maximum experimental and parametric SCFs for each joint

Specimen No.	Exp.	UEG	DnV	Gibstein	Soh
T1OPB	2.98	4.36	4.62	4.62	4.07
T2OPB	2.06	3.50	3.93	3.93	3.00
T3OPB	5.58	14.8	10.6	10.6	7.35
T4OPB	3.87	5.66	6.01	6.01	4.88
T5OPB	4.29	8.86	7.54	7.54	5.09
T6OPB	6.73	17.9	12.8	12.8	8.85

Table 4 Experimental fatigue life, N_3 normalised to 16 mm and 32 mm plate thickness

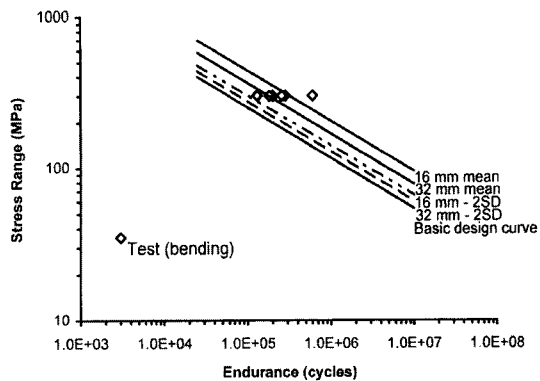| Specimen No.	$N_3 \times 10^5$ Experimental	$N_3 \times 10^5$ Normalised to 16 mm	$N_3 \times 10^5$ Normalised to 32 mm
T1OPB	2.82	1.98	1.18
T2OPB	5.65	3.97	2.36
T3OPB	2.01	1.00	0.59
T4OPB	2.56	1.80	1.07
T5OPB	1.66	1.17	0.69
T6OPB	1.83	0.91	0.54

Fig. 8 Fatigue life (N_3) of the CHS-to-RHS joints plotted vs. experimental hot spot stress range, and compared with DEn (Gurney, 1982) design S-N curves and associated scatter band for tubular joints
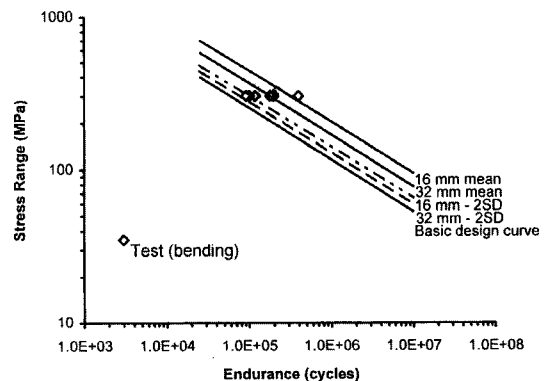
Fig. 9 Same experimental data N_3 as shown in Fig. 8 but normalised to 16 mm thickness using Eq. (2) and compared with DEn (Gurney, 1982) design S-N curves and associated scatter band for tubular joints

welded fabrications, and various design guidelines recommend different correction factors with respect to a reference thickness.

In order to correct for the thickness effect, the following equation (Gurney, 1991) was used in the present study,

$$N_t = N_o(t_o/t)^{0.75} \qquad (2)$$

where N_o is fatigue life for plate thickness t_o.

In Table 4 is presented the fatigue life N_3 normalized to 16 mm and 32 mm plate thickness using Eq. (2). The thickness correction is quite significant. The experimental fatigue data normalized to 16 mm thickness are shown in Fig. 9 for direct comparison with the DEn (Gurney, 1982) design curve and associated scatter band.

The mean value of N_3 is now below the mean S-N curve for 16 mm tubular joints. However, all the experimental data fall above the basic design S-N curve. It should be noted that the data base underlying Eq. (2) is from tests with plate thickness in the range 12 mm and above. The application of Eq. (2) for specimens with wall thickness in the range 6.3-10 mm is beyond the normal validity range for this equation. Most design codes do not allow for utilization of plate thickness below the reference thickness. However, van Wingerde (1992) advocated that the beneficial thickness effect is real down to the thickness in the range of 4 mm.

6. Conclusions

An experimental analysis for SCF measurement and fatigue behaviour of six different hollow section T-joints with circular braces and rectangular chords was presented. The measured SCFs for CHS-to-RHS joints were consistently below predictions by parametric equations derived for CHS-to-CHS joints. On the basis of measured hot spot stress the fatigue strength of the CHS-to-RHS joints was in reasonably good correspondence with the referred fatigue design guidance for tubular joints. Due to the combination of a simple welding geometry and an improved stress concentration factor compared to the CHS-to-CHS joints, the CHS-to-RHS joints may provide an optimum solution for some structural applications.

Acknowledgment

References

American Welding Society (AWS), 1998, Structural Welding Code : Steel, ANSI/AWS D1. 1-98, Miami, Fla. USA.

Bian, L. C. and Lim, J. K., 2001, "Fatigue Fracture Behaviour of Hollow Section Joints,"

Proceedings of the Conference of Korea Welding Society, 25-26 October, Ulsan, South Korea.

Chiew, S. P. and Soh, C. K., 2000, "Stress Concentrations at Intersection Regions of A Multiplanar Tubular DX-joint," *Journal of Constructional Steel Research*, Vol. 53, No. 2, pp. 225~244.

Department of Energy (DEn), 1990, Offshore Installation : Guidance on Design and Construction and Certification, Her Majesty's Stationery Office, London, UK.

Det norske Veritas (DnV), 1990, Rules for the Design, Construction and Inspection of Fixed Offshore Structures, Norway.

Gibstein, M. B. and Moe, E. T., 1985, Fatigue of Tubular Joints, Fatigue Handbook of Offshore Structures, Almar-Naess, A. (ed), Tapir, Trondheim, Norway, pp. 313~370.

Gurney, T. R., 1982, "The Basis of the Revised Fatigue Design Rules in the Department of Energy Offshore Guidance Notes," *Second International Conference on Offshore Welded Structures*, Cambridge, UK.

Gurney, T. R., 1991, The Fatigue Strength of Transverse Fillet Welded Joints. Abington Publishing, Cambridge, UK.

Radenkovic, D., 1981, "Stress Analysis in Tubular Joints," *Proceedings of International Conference of Steel in Marine Structures*, Institut de Recherches de la Siderurgie Francaise, Plenary Session, Paris, France, pp. 53~96.

Soh, A. K. and Soh, C. K., 1989, "SCF Equations for T/Y and K Square-to-Round Tubular Joints," *Journal of Petroleum Technology* (JPT), March, pp. 289~296.

Suh, M. W., Yang, W. H. and Suhr, J., 2001, "Analysis of the Joint Structure of the Vehicle Body by Condensed Joint Matrix Method," *KSME International Journal*, Vol. 15, No. 12, pp. 1639~1646.

UEG Publications, 1985, Design of Tubular Joints for Offshore Structures. UR33, London, UK.

van Wingerde, A. M., 1992, The Fatigue Behaviour of T- and X-joints Made of Square Hollow Sections. Heron, Vol. 37, No. 2, Delft, Netherlands.